

# Optimizing PID Values for Controlling Supply Air Temperature in AHU6

Daniel Pak, Ruben Solano

May 2021

# 1 Abstract

Air handling units (AHUs) are crucial in providing adequately treated air into occupied spaces. At 41 Cooper Square, there are several AHUs in operations to serve different spaces like laboratories or classrooms. The energy cost of these crucial pieces of equipment are often large, so it is important they are running efficiently. One of the units in the building, AHU6, currently has trouble controlling supply air temperature (SAT) effectively. There are several inputs into the system, from static pressure setpoint, to various kinds of actuation efforts by the heating, cooling, and reheat coils. The goal of this project is to model AHU6 as a first-order plant and recommend optimal gains or the PID controller that modulates the supply air temperature. The methodology to complete this task involved three phases. First, historical data was used to model AHU6 as a first-order plant. Then, the model was verified by inputting historical PID values and evaluating how well the model tracked the actual data from the building management system (BMS). Finally, these PID values were tuned to recommend optimal gains for the system, with special attention being given to stability and disturbance rejection.

## 2 Introduction

In 41 Cooper Square, the HVAC system is composed of a complex network of equipment. The various pieces of machinery, sensors, and actuators are controlled by the Building Management System (BMS). The BMS is responsible for taking measurements from sensors to identify the heating, cooling, and ventilation demands of the building, telling operators to determine the appropriate control efforts, and actuating the various pieces of equipment in order to meet those demands.

One example of equipment that the BMS controls is the air handling units (AHUs). An AHU is a device that takes outside air, filters it, heats or cools it, brings it to a desired humidity, and then supplies it to the building. In order to achieve temperature control, the AHUs at 41 Cooper Square use water-filled heating and cooling coils. For humidity control, the AHUs use humidifiers, although in this case, the AHU in question does not have a humidifier.

A screenshot of the BMS interface, courtesy of Professor Baglione's website [1], is shown below. It depicts AHU6, the chief point of interest for this report. This unit uses a fan to supply outside air to a damper that controls flow. The air is then heated or cooled depending on the temperature, reheated in order to dehumidify it, and then supplied to most of the classrooms in 41 Cooper Square. All along the way, there are various sensors that track temperature, flow, and static pressure.

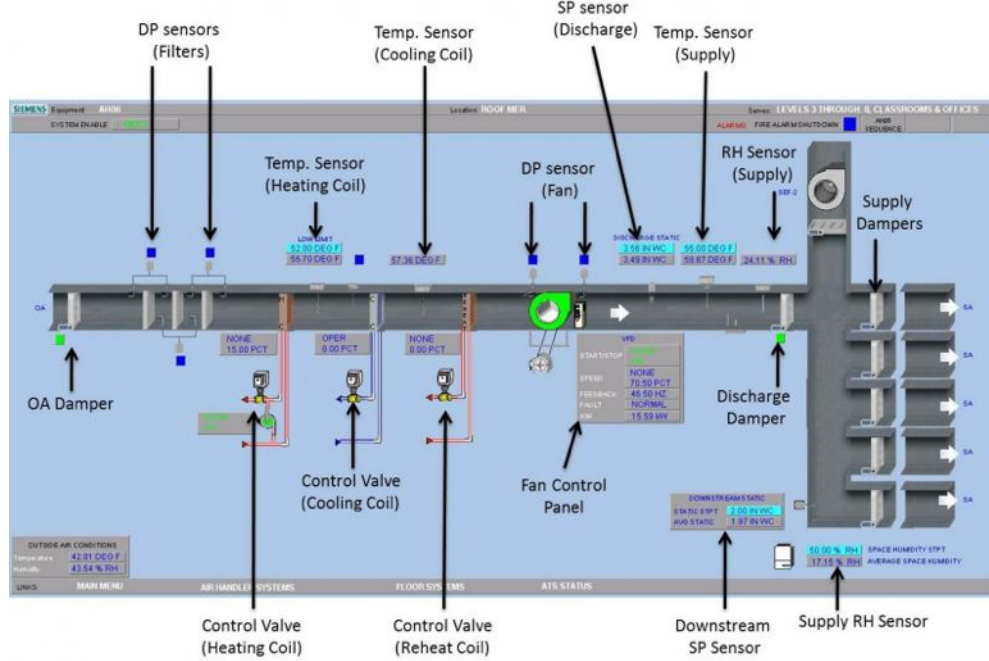


Figure 1: AHU6 Diagram

In order to give the control system commands, code must be written in the Powers Process Control Language (PPCL). This code is fed into the BMS and provides the instructions for how to control the various systems throughout the buildings [2]. Understanding how the BMS interprets instructions in PPCL was important in the analysis of AHU6.

Although Siemens makes the PPCL manual available for free, a few specific points in the manual were of interest in this project. For one, the bias value within the LOOP syntax was important to understand. The manual recommends the operator to calculate bias by adding 50% of the range of the output variable to the minimum value of the output variable. In the case of AHU6, the output variable from the controller is valve percent. The minimum value of the valve percent is 0%, and the range is 100%, so the recommended bias is 50%. However, the bias value can be set higher or lower depending on performance needs. When using PID control, it gives a starting point for control whenever the PID values are changed.

Another important point to note about the LOOP syntax is the difference between “pv” and “cv”. In PPCL, the “pv” refers to the process variable being controlled. In the case of AHU6, the process variable was supply air temperature. On the other hand, “cv” refers to an actuator signal that exerts a control effort on the system. In the case of AHU6, the signal was controlling the valve percentage.

The main objective is to perform analysis on AHU6 by creating a model and using controls techniques to have a simpler understand of how the system behaves.

### 3 Current BMS Data Analysis

The historical data for April 6th 2021 and April 11th 2021 is shown below in Figures 2 and 3. The data points were taken from the BMS at 15 minute intervals. There are some

interesting phenomena to note. For one, when the outside air temperature rises significantly past the temperature set point, the heating coil valve seems to automatically go to 0%. The supply air temperature then follows the outside air temperature almost perfectly. This is because the BMS is trying to stop heating the air and actuate the cooling coils instead. However, during this time the cooling coils were drained, and so there is no control effort at all. A second thing to note from this data is that the control system is very sensitive to disturbances. When the outside air temperature fluctuates very little, the BMS seems to control the supply air temperature effectively. This is exemplified in the data from April 11th. The outside air temperature fluctuates only about 2°F throughout most of the day, and the supply air temperature oscillates about 4°F. In contrast, when the outside air temperature experiences a large fluctuation, the BMS does not exhibit stable control. For example, on April 6th, the outside air changed by about 10°F in a relatively small amount of time, and the supply air temperature experienced oscillations with a magnitude of around 12°F.

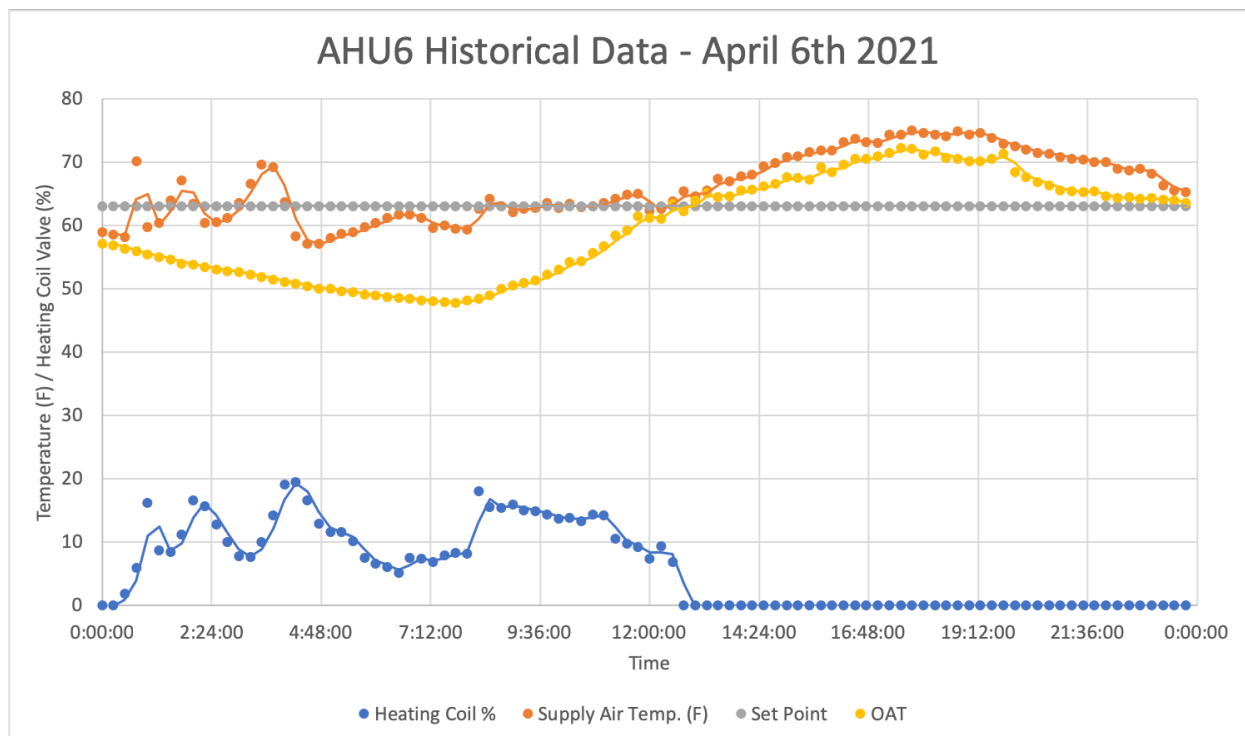


Figure 2: AHU6 Historial Data for April 6th 2021

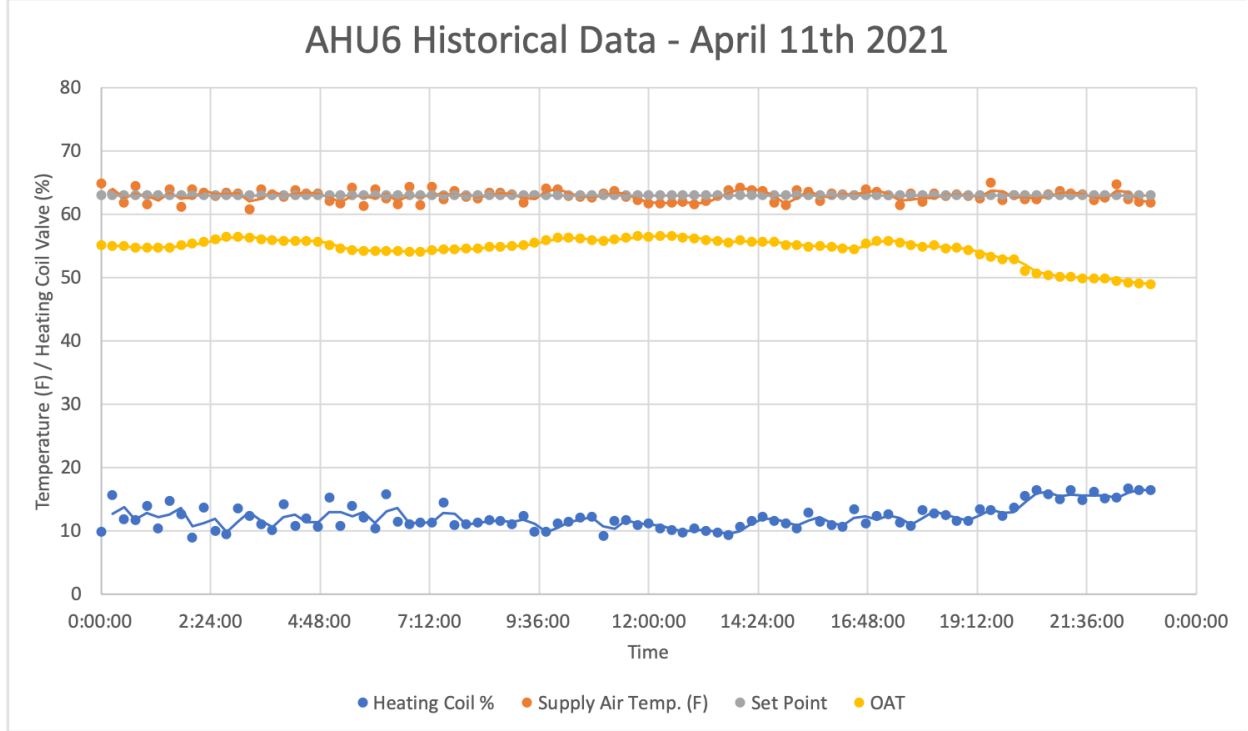


Figure 3: AHU6 Historial Data for April 11th 2021

## 4 Assumptions

The assumptions to model AHU6 are as follows.

1. The air damper position at a constant position
2. Outside air temperature (OAT) is at a constant temperature
3. Air flow entering AHU6 is constant
4. The static pressure setpoint is at a constant value of 2" WC during the day
5. The desired setpoint supply air temperature (SAT) is dependent on the wet bulb temperature of the outside air
6. The actuation effort is only done by the heating coil as the cooling coil is drained to prevent freezing during the winter season

The assumptions for the controls analysis are as follows.

1. All signals are continuous and not assumed to be quantized by the sampling rate, which by default on the BMS is 15 minutes

2. The system is single input, single output (SISO), where the desired setpoint SAT is the input and the measured SAT is the output
3. From the actual design specifications of the BMS, the controller for AHU6 MUST be PID
4. Derivative control does not require a low pass filter, which is typically used to reduce high frequency noise
5. The feedback control diagram is as follows and follows the method from the Siemens PPCL book

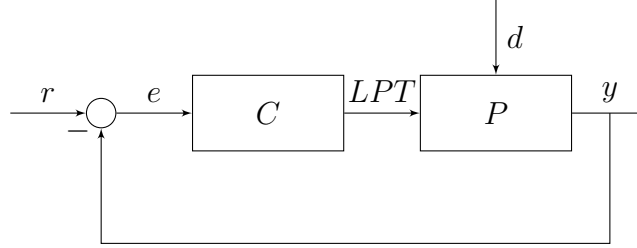


Figure 4: Feedback Block Diagram of AHU6

where  $P$  is AHU6,  $C$  is the controller,  $r$  is the SAT setpoint,  $y$  is the actual SAT,  $d$  is a disturbance,  $e$  is the error, and LPT (Loop Out) is the heating coil valve percent.

## 5 Plant Model

AHU6 was modelled as a first order system with a time delay. This time delay is introduced as AHU6 is a thermal system and that the current temperature sensor measuring the temperature records the temperature of the air after it passes through the coils.

The canonical form of a first order system with a time delay is as follows.

$$P(s) = \frac{K}{\tau s + 1} e^{-s\theta} \quad (1)$$

where  $K$  is the DC gain of the system,  $\tau$  is the time constant of the system, and  $\theta$  is the time delay of the system. These parameters can all be determined by inputting a step response into the plant and seeing the open-loop response, which does not involve a controller or feedback. The block diagram is shown in Figure 5.

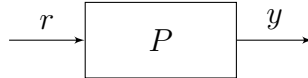


Figure 5: Open Loop Block Diagram

In Figure 5, the input  $r$  is a change in the heating coil valve, with the output  $y$  being the SAT. Data was plotted from 2/24/2021, where it was known that a step change occurred.

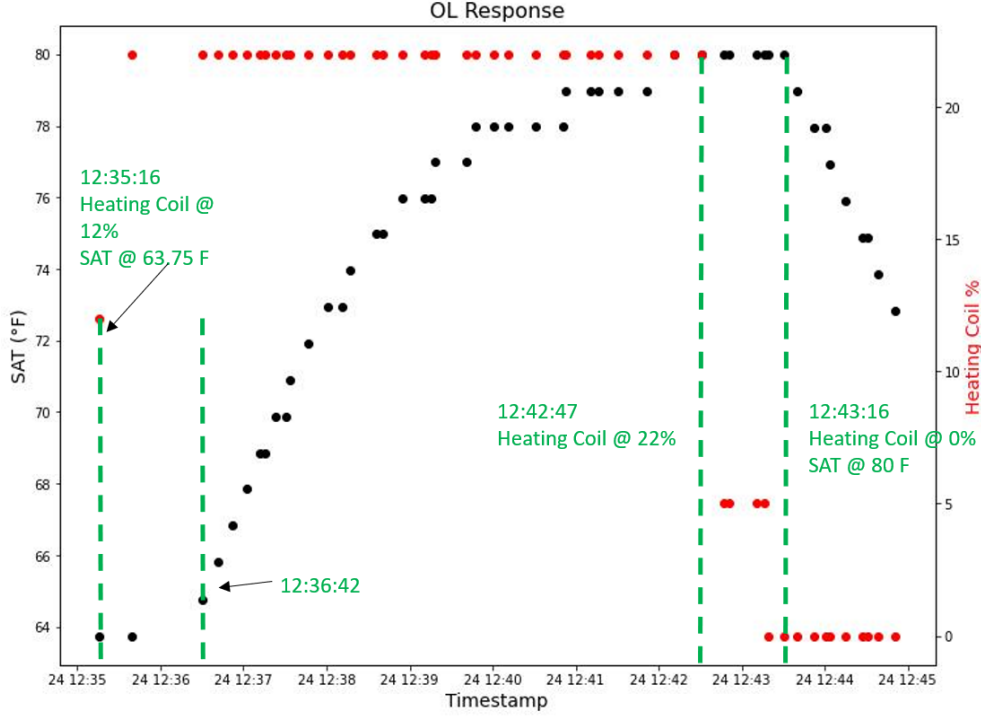


Figure 6: Open Loop Step Response of Data on 2/24/2021

In Figure 6, the step change in the heating coil valve was from 12% to 22%, which is a change in input of 10%. The gain  $K$  can be calculated by knowing the temperature before the step was inputted  $T_i$  and the steady state temperature after the step was inputted  $T_{ss}$ . This is calculated as follows.

$$K = \frac{T_{ss} - T_i}{U_{ss} - U_i} = \frac{80^\circ F - 63.75^\circ F}{22\% - 12\%} = 1.625 \frac{^\circ F}{\%} \quad (2)$$

The time constant  $\tau$  can be calculated by knowing what how much time elapsed, with  $t = 0$  as when the step was inputted, when the temperature reached 63% of the value between  $T_i$  and  $T_{ss}$ . This value is calculated as

$$0.63 * (T_{ss} - T_i) + T_i = 0.63 * (80^\circ F - 63.75^\circ F) + 63.75^\circ F = 73.9875^\circ F \quad (3)$$

The amount of time elapsed from when the step input was inputted to the temperature of  $73.9875^\circ F$  was calculated to be 173 s.

The time delay  $\theta$  can be calculated by knowing how much time elapsed, with  $t = 0$  as when the step was inputted, when the temperature changed from its initial value of  $T_{ss}$ . This was calculated to be 86 s.

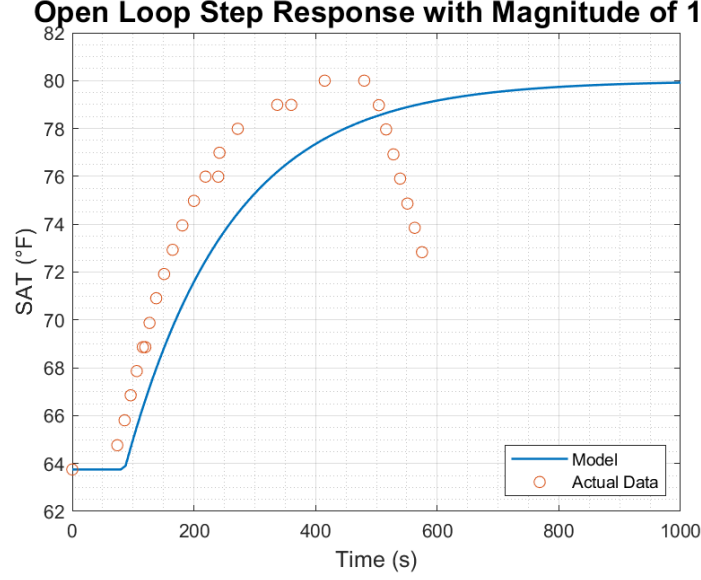


Figure 7: Open Loop Step Response Between Data and Model for 2/24/2021

Figure 7 shows the comparison between the actual data and the proposed first order model with a time delay plotted against each other. The actual data has a faster rise time than the proposed model, and achieves the final steady state value of  $80^{\circ}F$  faster. The model and data agree in the time delay as indicated when  $t = 86$ . Overall, this model is a good first order approximation of the complex AHU6 and was analyzed further.

## 6 Modeling a Time Delay

A time delay in the Laplace domain is represented by  $e^{-s\theta}$ . However, having this form in the Laplace domain is not easily understood as to how it changes the plant and also introduces computational concerns with a continuous time system in MATLAB, so the Padé Approximation is used. The Padé Approximation can represent a function as the ratio of 2 power series. Some low order approximations for  $e^{-s\theta}$  are as follows.

$$\begin{aligned} exp_{0,0}(-s\theta) &\approx 1 \\ exp_{1,1}(-s\theta) &\approx \frac{2 - s\theta}{2 + s\theta} \\ exp_{2,2}(-s\theta) &\approx \frac{s^2\theta^2 - 6s\theta + 12}{s^2\theta^2 + 6s\theta + 12} \end{aligned}$$

Some plots are shown below depicting the accuracy of the Padé Approximation for  $e^{-s\theta}$  using the above approximations.



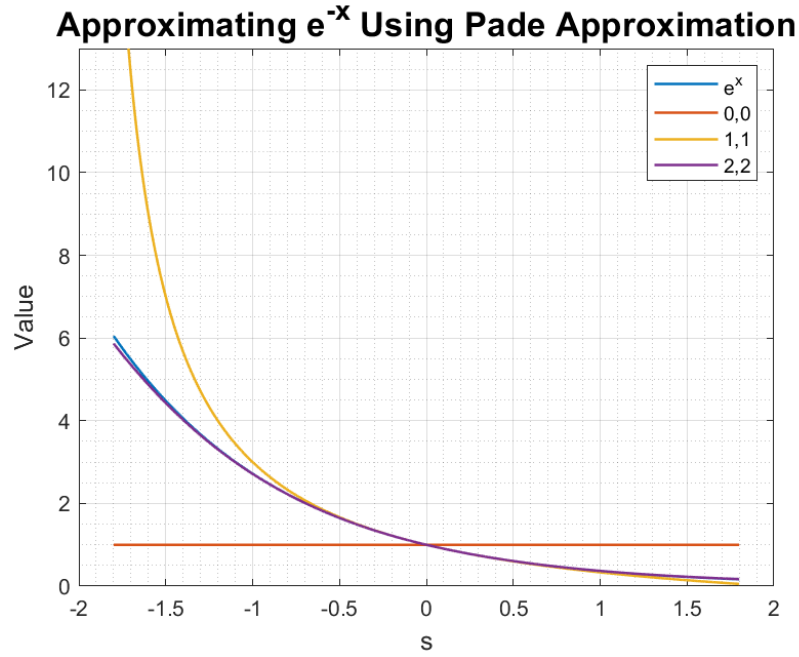


Figure 8: Approximating  $e^{-x}$  with Padé Approximation

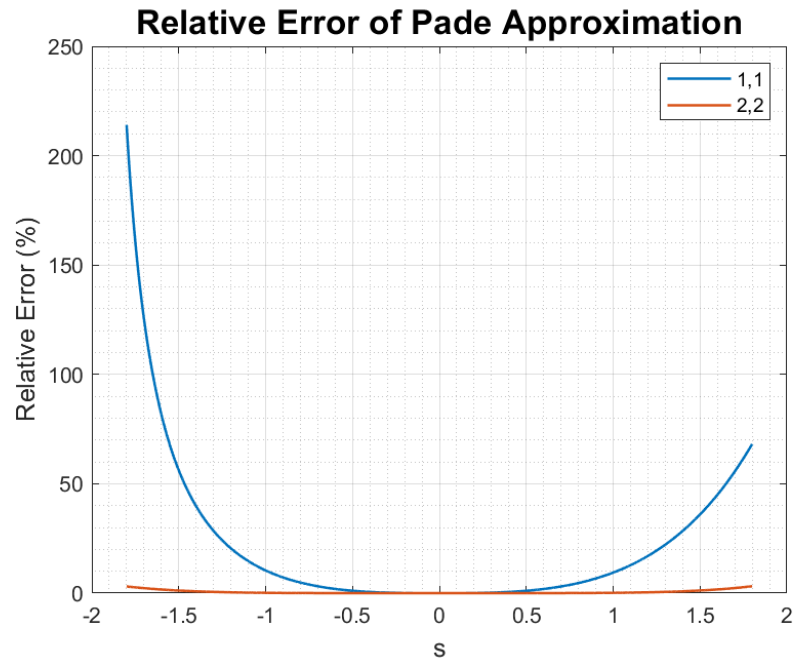


Figure 9: Relative Error of Padé Approximation

As expected, a higher order Padé Approximation will result in a lower relative error and also work for a larger band of frequencies  $s$ . However, using a higher order Padé

Approximation results in increasing the number of poles and zeros in a system based on the order of the approximation. Using a 0th order approximation adds nothing new. A 1st order approximation adds a pole at  $-\frac{2}{\theta}$  and a zero at  $\frac{2}{\theta}$ .

## 7 Root Locus

The root locus is a graphical representation of how the open loop poles and zeros affect the location of the closed loop poles. The formula to calculate the root locus is as follows:

$$1 + KP(s)C(s) = 0 \quad (4)$$

where  $P(s)$  is the plant,  $C(s)$  is the controller, and  $K$  is the gain. Increasing  $K$  to a large value can result in closed loop instability, however this is not known until the root locus method is performed.

For the plant without a time delay, it is represented as follows.

$$P(s) = \frac{K}{\tau s + 1} \quad (5)$$

Using the values from Section 5, the root locus can be determined and plotted in MATLAB for 5 with a P, PI, and PID controller. However, what is important is that for a PI and PID controller, there are multiple gains, which the root locus cannot solve for simultaneously. Therefore, each controller must be rewritten to hold some values fixed.

In the case of a PI controller, the canonical form can be rewritten as follows:

$$C_{PI}(s) = K_p + \frac{K_i}{s} = K_p \frac{s + \frac{K_i}{K_p}}{s} \quad (6)$$

In Equation 6,  $\frac{K_i}{K_p}$  is held constant, while  $K_p$  is the gain that will be changed using root locus.

In the case of a PID controller, the canonical form can be rewritten as follows:

$$C_{PID}(s) = K_p + \frac{K_i}{s} + K_d s = K_d \frac{s^2 + \frac{K_p}{K_d} s + \frac{K_i}{K_d}}{s} \quad (7)$$

In Equation 7,  $\frac{K_p}{K_d}$  and  $\frac{K_i}{K_d}$  are held constant, while  $K_d$  is the gain that will be changed using root locus.

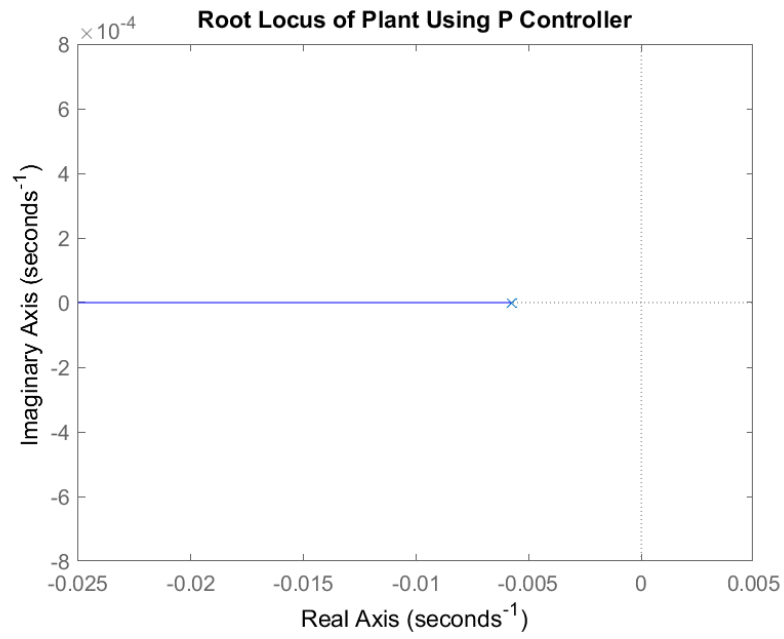


Figure 10: Root Locus of the Plant with No Delay using P

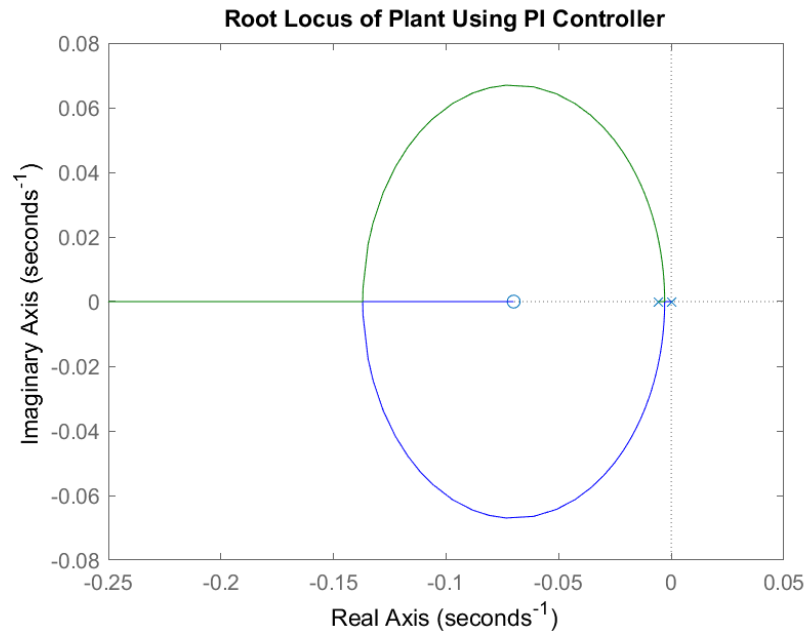


Figure 11: Root Locus of the Plant with No Delay using PI

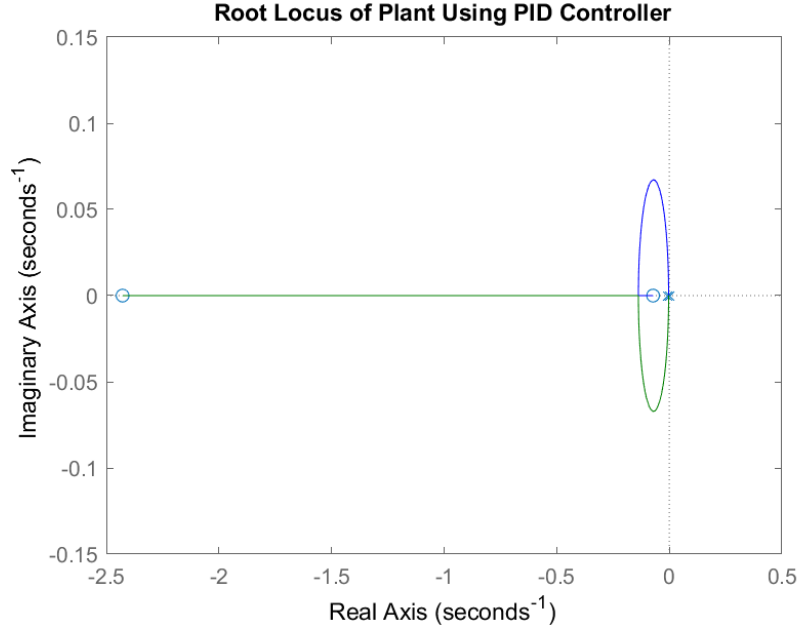


Figure 12: Root Locus of the Plant with No Delay using PID

In Figure 11,  $\frac{K_i}{K_p}$  was set as  $\frac{3.5}{50}$ . In Figure 12,  $\frac{K_p}{K_d}$  was set as  $\frac{50}{20}$  while  $\frac{K_i}{K_d}$  was set as  $\frac{3.5}{20}$ . These values for P, I, and D were based off gains in the BMS on 1/13/2021. As expected, all of these figures show that the gain for an ordinary first order system can be increased infinitely with no instability as the entire root locus resides in the left half plane.

The closed loop response and disturbance rejection are shown below using the original gains of  $P = 50$ ,  $I = 3$ , and  $D = 20$ .

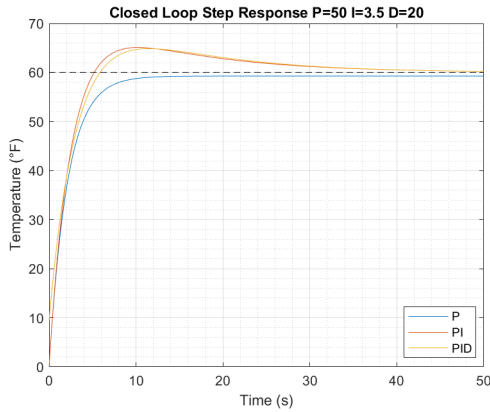


Figure 13: Closed Loop Step Response

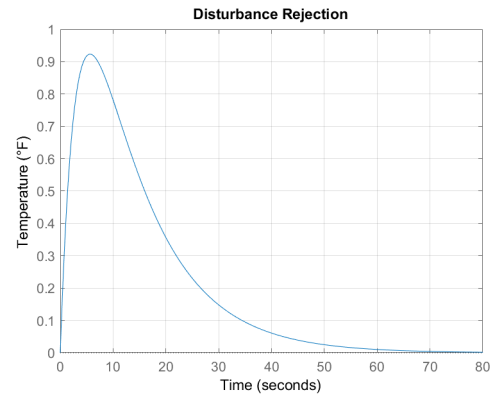


Figure 14: Disturbance Rejection

As expected, Figures 13 and 14 verify that the system is closed loop stable with the prescribed gains. The PID controller actuates the plant to reach the setpoint of 60°F and

will always reject the step disturbance.

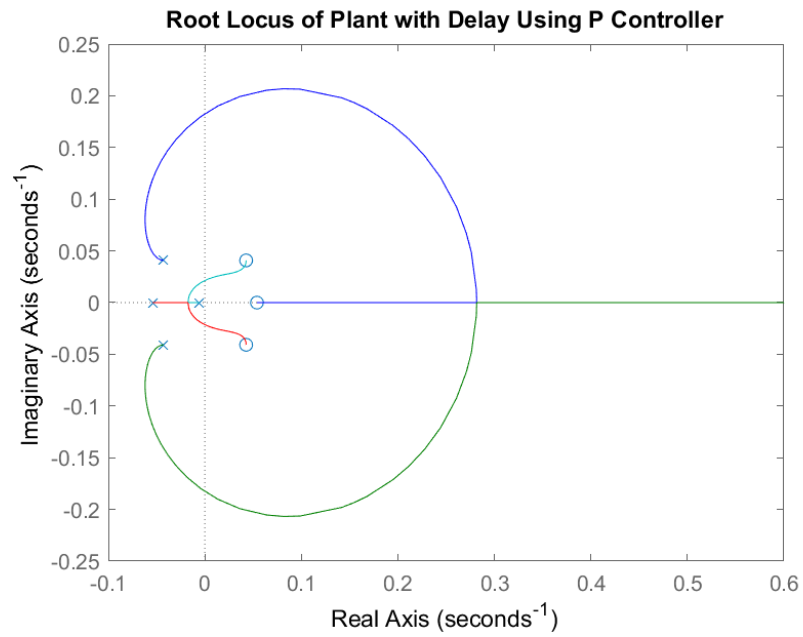


Figure 15: Root Locus of the Plant with Delay using P

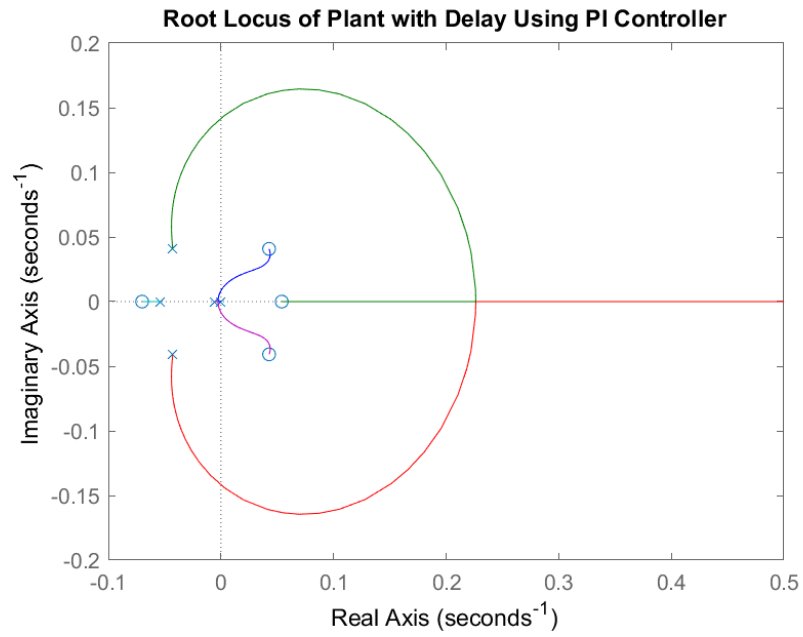


Figure 16: Root Locus of the Plant with Delay using PI

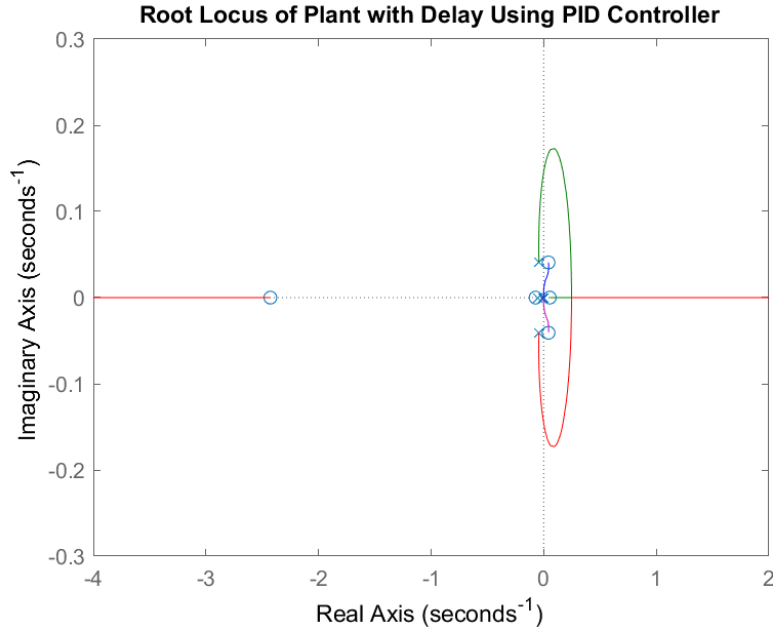


Figure 17: Root Locus of the Plant with Delay using PID

In Figures 15, 16, and 17, these plants utilized the same gain ratios as the previous 3 root locus plots, but included the time delay of 86 seconds using a 3rd order Padé Approximation, which introduces 3 poles and 3 zeros.

In Figure 15, the gains that make the system marginally stable are 19.3 and 2.7. In Figure 16, the gains that make the system marginally stable are 13.2 and 0.132. In Figure 17, the gains that make the system marginally stable are 5.73 and 0.0523. From these values, the lower one are used to introduce a maximum on the allowable gain.

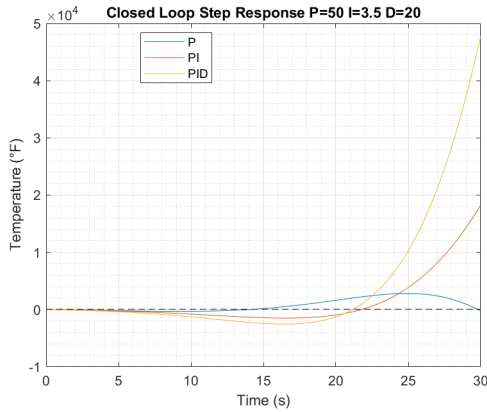


Figure 18: Closed Loop Step Response with Delay using BMS Gains

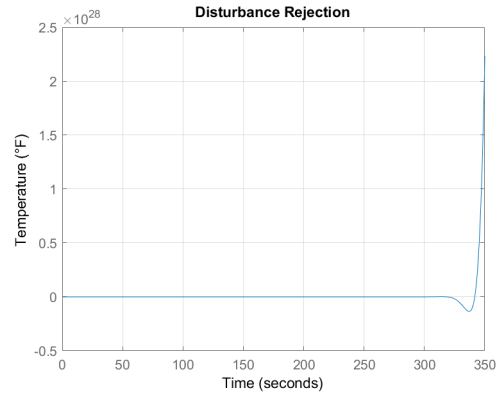


Figure 19: Disturbance Rejection with Delay using BMS Gains

As expected, Figures 18 and 19 verify that the system is closed loop unstable with the prescribed gains in the BMS. The closed loop step response and the disturbance rejection plots were replotted using a new set of gains that the root locus indicated are closed loop stable, which are  $P = 0.05$ ,  $I = 0.0035$ , and  $D = 0.02$ , the original gains divided by 1000.

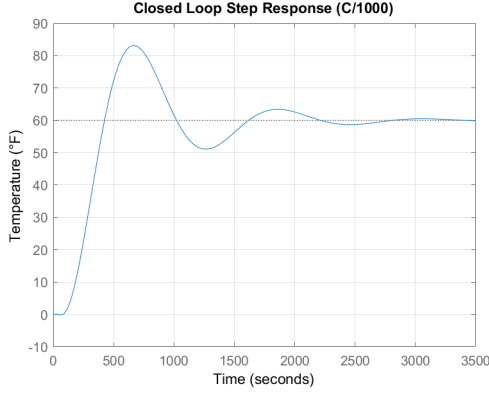


Figure 20: Closed Loop Step Response with Delay using New Gains

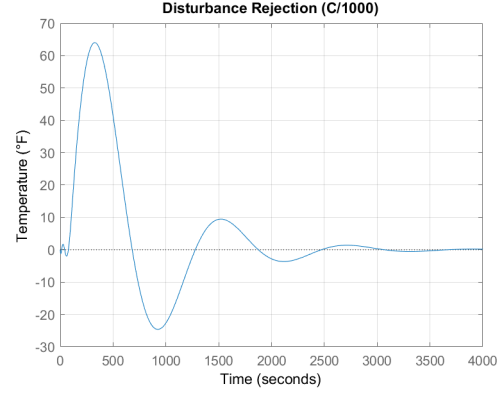


Figure 21: Disturbance Rejection with Delay using New Gains

Figures 20 and 21 show that with the changed gains, the closed loop response will successfully track the setpoint SAT, and reject the disturbance. However, there must be a better way to determine optimal gains without relying on the first order plant with no time delays.

## 8 PID Tuning

To obtain an optimal PID controller, internal model control (IMC) was used to tune the plant with the time delay.

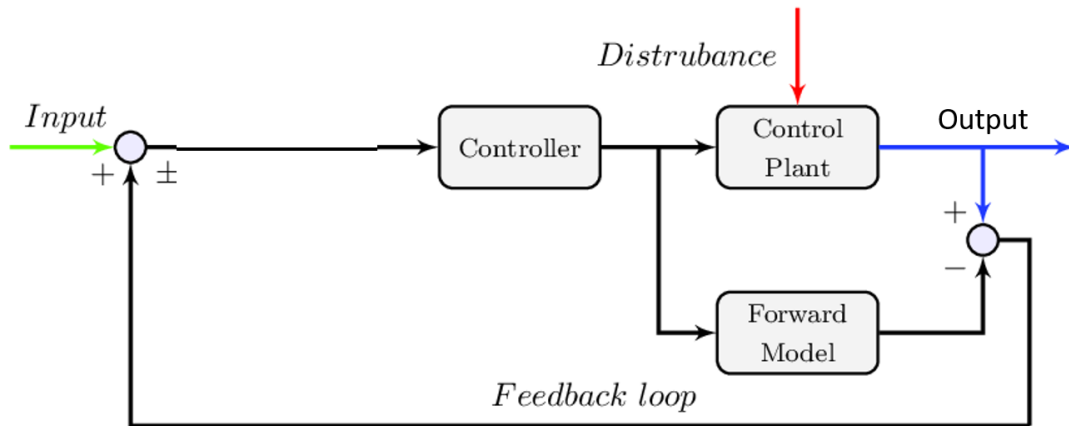


Figure 22: IMC Block Diagram

IMC tries to specify the desired closed-loop response and solve for the optimal controller [3], while also being robust for disturbance rejection. Instead of a heuristic approach like Ziegler-Nichols, IMC can be used to determine the best  $P$ ,  $I$ , and  $D$  by solving for it directly. Figure 22 shows the difference of using IMC instead of regular PID feedback, where instead there is a forward model to correct for the error fed in to the controller. IMC can approximate complicated plants with many poles and zeros to a single first order plant with 1 pole and a time delay.

Generally, tuning rules created by IMC for a PID controller use a rewritten form of the PID controller which is

$$C_{PID}(s) = K_c \left( 1 + \frac{1}{\tau_i s} + \tau_d s \right) \quad (8)$$

where  $K_c$  is the controller gain,  $\tau_i$  is the integral time and  $\tau_d$  is the derivative time. IMC tries to solve for these 3 terms by tuning for a parameter  $\tau_c$ , the filter coefficient. This coefficient  $\tau_c$  gives a good balance between the PID coefficients and can be adjusted to get a trade-off between performance and robustness.

For a first order system with a time delay, there are a set of tuning rules called simple IMC (SIMC) [3] which states

$$K_c = \frac{1}{K} \frac{\tau}{\tau_c + \theta} \quad \tau_i = \min(\tau, 4(\tau_c + \theta)) \quad (9)$$

Note, Equation 9 does not required a derivative term in the PID controller, resulting in a PI controller. The gains are determined below.

Table 1: Gains Calculated Using SIMC

$\tau_c$	$K_p$	$K_i$
1	1.2237	0.0071
10	1.1090	0.0064
100	0.5724	0.0033

There is also improved SIMC [4] which states

$$K_c = \frac{1}{K} \frac{\tau + \frac{\theta}{3}}{\tau_c + \theta} \quad \tau_i = \min(\tau + \frac{\theta}{3}, 4(\tau_c + \theta)) \quad (10)$$

Again, Equation 10 does not required a derivative term in the PID controller, resulting in a PI controller. When substituting values from the first order plant model using SIMC and Improved SIMC, all the  $K_i$  remained the same for the same  $\tau_c$ . The gains are determined below.

Table 2: Gains Calculated Using Improved SIMC

$\tau_c$	$K_p$	$K_i$
1	1.4265	0.0071
10	1.2927	0.0064
100	0.6672	0.0033



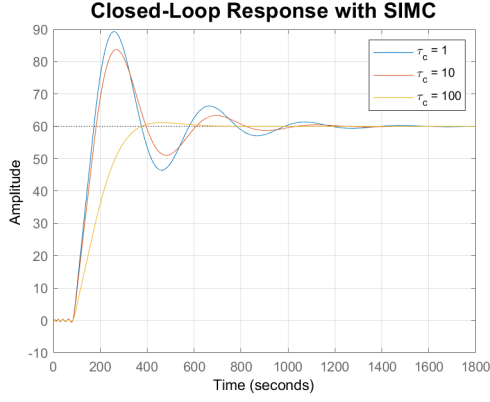


Figure 23: Closed Loop Response Using SIMC

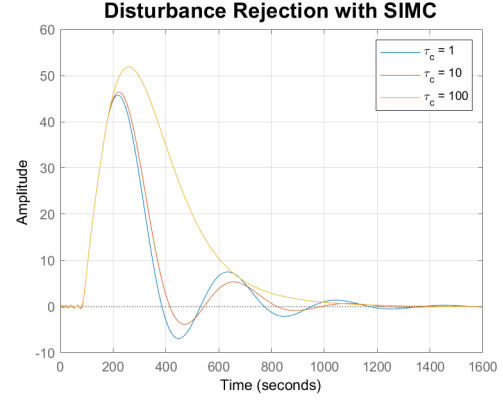


Figure 24: Disturbance Rejection Using SIMC

Table 3: Step Response Characteristics Using SIMC for Closed Loop Response

$\tau_c$	$t_{rise}$	$t_{settling}$	% overshoot
1	69.3	1100.4	48.9
10	76.5	927.5	39.6
100	187.2	348.2	1.9184

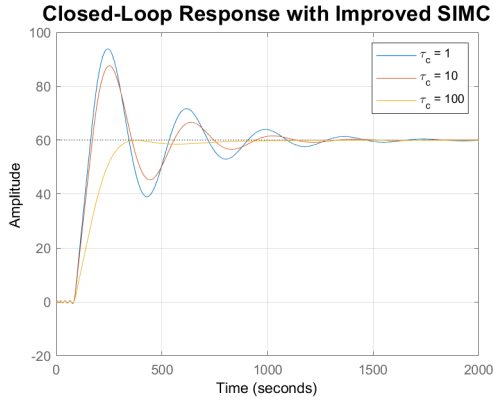


Figure 25: Closed Loop Response Using Improved SIMC

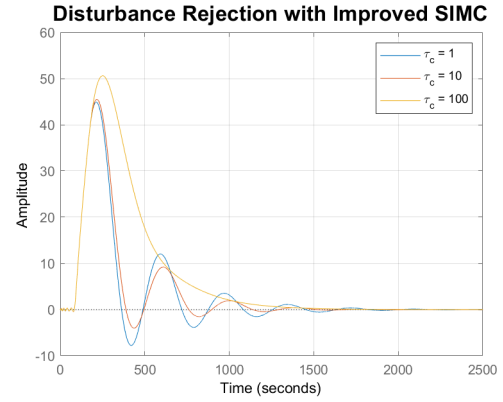


Figure 26: Disturbance Rejection Using Improved SIMC

Table 4: Step Response Characteristics Using Improved SIMC for Closed Loop Response

$\tau_c$	$t_{rise}$	$t_{settling}$	% overshoot
1	61.2	1390.3	56.5
10	67.6	1069.0	46.0
100	163.1	660.4	0

For the total of 6 cases, it is apparent that using Improved SIMC with  $\tau_c = 100$  performed the best and is the most robust, even though it is a PI controller. The overshoot was minimal and the settling time was low, even with a high rise time. In all cases, the input disturbance was completely rejected. In the case for  $\tau_c = 100$ , it gradually decreased to an amplitude of 0, while for  $\tau_c = 1$  and  $\tau_c = 10$ , the disturbance response exhibited sinusoidal behavior. From this analysis, the optimal gains for AHU6 are  $K_p = 0.6672$ ,  $K_i = 0.0033$ , and  $K_d = 0$ .

## 9 Discussion

With the optimal gains determined, what needs to be determined is if the results are sensible.

As this analysis assumed an ideal system, there was no consideration to the available bandwidth with sensors or with the data signals being quantized, as everything is assumed to be continuous signals. Available bandwidth is the limitation to how well one can capture or measure data. For example, your eyes have a refresh rate of 30 Hz to 60 Hz, which would limit you to be unable to view something at 120 Hz. However, the one factor that leads to a limitation to the bandwidth is the existence of the time delay of 86 seconds.

A good design specification is for a desired loop shape of  $L = PC$  to have a slope of -1 at the gain crossover frequency [3]. This is synonymous to an integrator which decreases in magnitude at a rate of -1, and decreases the phase by  $-90^\circ$ . Another design specification is having a phase margin of at least  $35^\circ$ . From these two conditions, the allowable phase is  $-55^\circ$  at the gain crossover frequency. Having a time delay results in a lag in the phase in the s-domain. To convert domains between s and  $i\omega$ ,  $e^{-s\theta} = e^{i\omega\theta}$ . The phase of  $e^{i\omega\theta}$  is just  $-\omega\theta$ , which is what is added to the phase on a Bode Plot. However, if  $\omega = \frac{1}{\theta}$ , then the additional phase is -1 rad, which is  $-57^\circ$ . Therefore, comparing the allowable phase to the additional phase that is being contributed to the system (which is fairly close), a bandwidth consideration for acceptable control performance states that

$$\omega_c < \frac{1}{\theta} \quad (11)$$

For AHU6,  $\omega_c < 0.0731 \frac{rad}{s}$ . Analyzing the Bode Plot for the chosen controller in Figure 27, still with a Padé Approximation of order 3, it shows that all of the design specifications were met. There is sufficient phase margin of  $65.6^\circ$  and the gain crossover frequency is  $0.00584 \frac{rad}{s}$ . The slope of the magnitude at the gain crossover frequency is also -1, showing how effective Improved SIMC is.

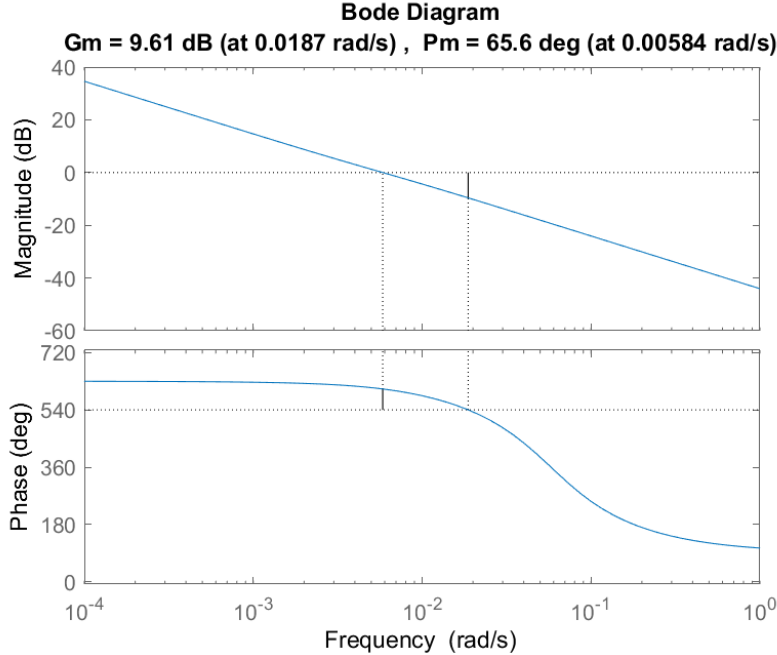


Figure 27: Bode Plot for Improved SIMC with  $\tau_c=100$

Another important question is whether this chosen set of gains can be used on the BMS to control AHU6. The results are 2 orders of magnitude smaller than the prescribed gains obtained from the BMS for a typical day. Not only that, but Improved SIMC does not require derivative control. The benefits of derivative control are reducing overshoot and having a faster response time, but can amplify noise and cause instability. In reality, this is something that would be applicable for a real system.

What is currently being done by operators for AHU6 is changing the PID gains to see the response, through previous knowledge of how the BMS reacted to certain gains.

In Figure 28, the gains used are P=50, I=2, and D=10. This resulted in the SAT having sustained oscillations between 55°F and 75°F, compared to the setpoint SAT of 62°. This is not desired behavior, as the system is marginally stable for these set of gains, indicating that P and D are too high.

In Figure 29, the gains used are P=140, I=3, and D=0. One thing to note is that the sampling rate for this data was at every 15 minutes. However, even with the low sampling rate, it is apparent that the amplitude of the SAT was increasing compared to the setpoint SAT of 63°. For these gains, the system is clearly unstable, showing the consequences of having too high of a proportional gain with no derivative gain to reduce overshoot and have a faster response time.

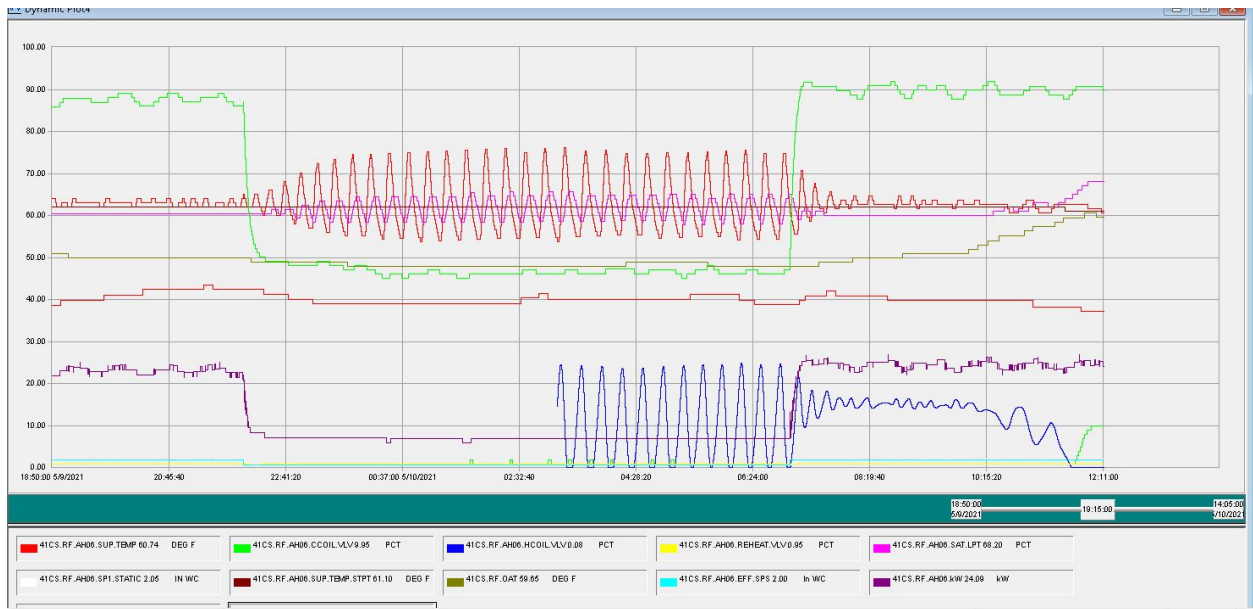


Figure 28: Recorded Data on May 10th 2021 with P=50, I=2, D=10

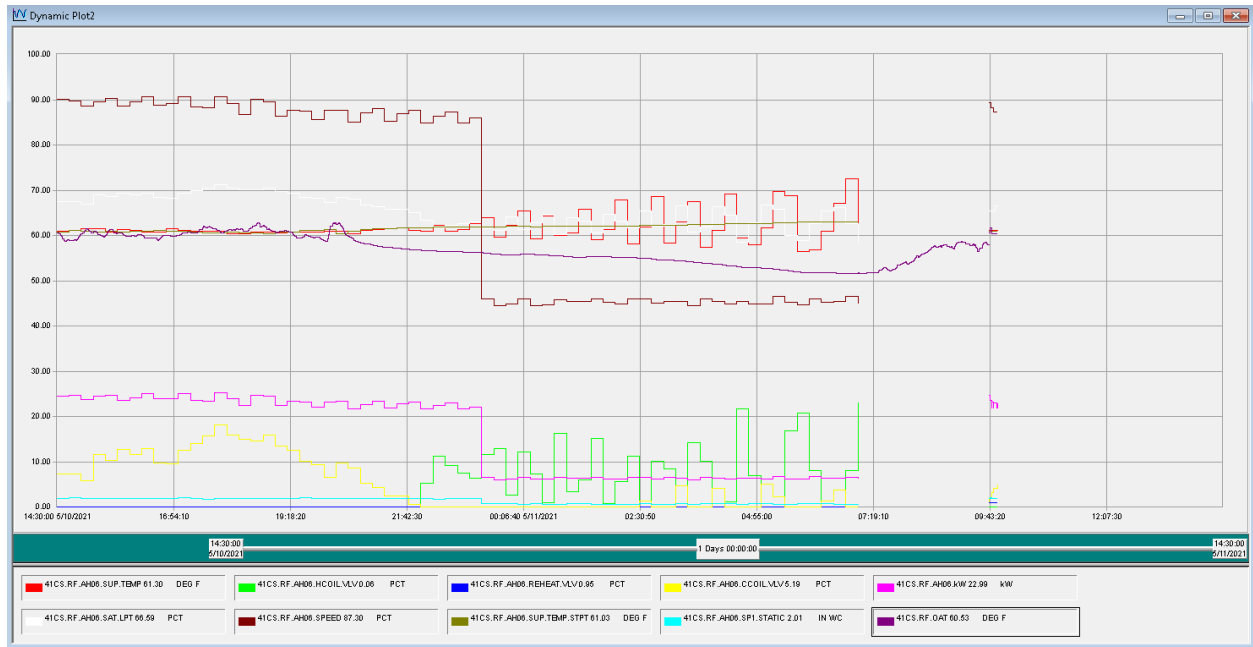


Figure 29: Recorded Data on May 11th 2021 with P=140, I=3, D=0

## 10 Future Work

The most logical step to take is to implement the gains found by using Improved SIMC, even if they are significantly smaller, for a short time and see how the actual response compares with the model at a high sampling rate. The controls structure in the PPCL Code for the BMS could also be changed to not just use PID controls, but instead other methods like loop-shaping or  $\mathcal{H}_\infty$ . The model can also be expanded to be a MIMO (multiple input, multiple output) system to see how other unmodeled aspects affect the SAT, or the original SISO model can be kept, but instead as a higher order model using more data from the BMS.

## References

- [1] Melody Baglione. Air handling units.
- [2] *APOGEE Powers Process Control Language (PPCL) User's Manual*, pages 4–47–4–53. Siemens Building Technologies, Inc.
- [3] Sigurd Skogestad and Ian Postlethwaite. *Multivariable feedback control: Analysis and Design*. John Wiley, Hoboken, US-NJ, 2005.
- [4] Sigurd Skogestad and Chriss Grimholt. The simc method for smooth pid controller tuning. *Advances in Industrial Control*, pages 147–175, 01 2012.